ELSEVIER

Contents lists available at ScienceDirect

Journal of Magnetism and Magnetic Materials

journal homepage: www.elsevier.com/locate/jmmm





Low damping at few-K temperatures in $Y_3Fe_5O_{12}$ epitaxial films isolated from $Gd_3Ga_5O_{12}$ substrate using a diamagnetic $Y_3Sc_{2.5}Al_{2.5}O_{12}$ spacer

Side Guo, Brendan McCullian, P. Chris Hammel, Fengyuan Yang

Department of Physics, The Ohio State University, Columbus, OH 43210, United States

ABSTRACT

 $Y_3Fe_5O_{12}$ (YIG) thin films are typically grown on $Gd_3Ga_5O_{12}$ (GGG) substrates; however, such YIG thin films typically suffer from significantly increased damping at low temperatures due to the interfacial exchange coupling between the YIG magnetization and the lossy Gd^{3+} moments in GGG. To overcome this problem, we grow high-quality epitaxial YIG(35 nm) films on a thin diamagnetic $Y_3Sc_{2.5}Al_{2.5}O_{12}$ (YSAG) bilayer on GGG, where the YSAG buffer layer eliminates the exchange coupling between YIG and GGG. As a result, we obtain a much-improved damping of 1.2×10^{-3} at 2–5 K.

1. Introduction

Spin waves, also referred to as magnons, are an essential part of magnonics and spintronics [1-8] as these magnetic excitations can be utilized for the manipulation and transmission of information. As a magnetic insulator, yttrium iron garnet (Y₃Fe₅O₁₂, YIG) is one of the lowest damping materials [9] and has received tremendous attention for fundamental studies and device applications. For example, its low damping leads to long spin relaxation length which makes it a good medium for spin-wave propagation. We previously reported growth of epitaxial YIG films on Gd₃Ga₅O₁₂ (GGG) substrates using off-axis sputtering, which exhibit very low Gilbert damping of 6.1×10^{-4} at room temperature [10]. However, the ferromagnetic resonance (FMR) linewidth of the YIG films increases significantly as temperature decreases, indicating enhanced damping at low temperatures (<100 K) [11]. The larger damping in YIG thin films at cryogenic temperatures limits their low temperature application such as in magnonics and magnon-based quantum information science (QIS) [12,13]. If the damping can be reduced to a very low level near 1 K or below, YIG thin films will provide an excellent platform for magnonics and QIS studies. There has been active ongoing research about the coupling between bulk YIG and microwave resonators, such as cavity and coplanar waveguide [12-15], but planar YIG films that can be readily incorporated in large scale fabrication will be an attractive platform. In addition, metallic ferromagnetic films with high saturation magnetization and very low damping are also promising for low-temperature QIS applications [16], which is beyond the scope of this work.

To probe the underlying mechanisms responsible for the increased damping in YIG/GGG thin films at low temperatures, we first look at the

widely-used Landau-Lifshitz-Gilbert (LLG) equation which describes the resonance dynamics of a magnetic material [17]:

$$\frac{d\overrightarrow{M}}{dt} = -\gamma \overrightarrow{M} \times \overrightarrow{H}_{eff} + \frac{\alpha}{M_s} \overrightarrow{M} \times \frac{d\overrightarrow{M}}{dt} (cgs)$$
 (1)

where γ is the gyromagnetic ratio, α is a phenomenological coefficient that governs the rate of the damping, $M_{\rm S}$ is the saturation magnetization and $\overrightarrow{H}_{\rm eff}$ is the effective field that is a combination of the external magnetic field and the anisotropy field. This classic model is intuitive but does not reveal the sources of energy dissipation. In general, it is believed that there are several mechanisms contributing to the relaxation of YIG, either in bulk form or thin films. In the few-K to room temperature range, some of the most commonly mentioned ones are magnon-magnon scattering at interfacial defects [11] and relaxation through rare-earth impurities and/or Fe²⁺ defects [11,18–20].

However, as the YIG film thickness is reduced toward 10's or even several nm, the interfacial interactions between YIG and GGG become increasingly important. At low temperatures, the paramagnetism of the frustrated magnet GGG increases strongly and the interfacial magnetic coupling between the YIG magnetization and the Gd³⁺ moments serves as the dominant relaxation source in YIG, causing a significant increase in the damping of YIG thin films [11,21]. There have been reports of removing the GGG substrate after the YIG deposition [22,23], where the linewidths of YIG thin films are improved. However, such removal of the substrate requires extraordinary efforts and the free-standing YIG thin film is quite fragile. For the purpose of scalable device fabrication, a different approach of eliminating or weakening the relaxation of the YIG thin film by the GGG substrate is desired.

E-mail address: yang.1006@osu.edu (F. Yang).

^{*} Corresponding author.

Herein, we exploit the absence of paramagnetism in (diamagnetic) $Y_3Sc_{2.5}Al_{2.5}O_{12}$ (YSAG; Y^{3+} , Sc^{3+} , and Al^{3+} ions are all non-magnetic), which has the same garnet structure with a lattice constant close to those of GGG and YIG, to serve as a buffer layer for the growth of YIG thin films. A high-quality epitaxial YIG film can grow on YSAG-buffered GGG substrate while the magnetic moments of the YIG film and GGG are decoupled. As a result, we observe significantly narrower FMR linewidths and lower damping in the YIG/YSAG/GGG samples at low temperatures, as compared to those of YIG films directly on GGG.

2. Experimental methods

YIG and YSAG thin films were epitaxially grown on GGG (111) single crystal substrates using off-axis magnetron sputtering [10]. The YIG and YSAG sputtering targets are cold pressed using phase pure garnet nano powders synthesized by a sol–gel method [24] with Y₂O₃, Fe₂O₃, Sc₂O₃ and Al(NO₃)₃·9H₂O as the starting materials. The GGG (111) substrates were purchased from MTI Corporation. The bulk lattice constant of the Y₃Sc_{2.5}Al_{2.5}O₁₂ powder is a=12.344 Å, which has a small lattice mismatch of -0.3% (tensile strain) with GGG (a=12.383 Å), while YIG has a mismatch of only -0.06% (a=12.376 Å). The sputtering gas is a mixture of Ar and O₂ with a total pressure of 11.5 mTorr. The substrate temperature is 800°C and 650°C for YSAG and YIG deposition, respectively.

The quality of the YIG and YSAG films as well as YIG/YSAG bilayers is characterized by X-ray diffraction (XRD) and X-ray reflectivity (XRR), as shown in Fig. 1a and 1b. The well-defined (444) peaks and their clear Laue oscillations indicate highly coherent crystalline ordering of the

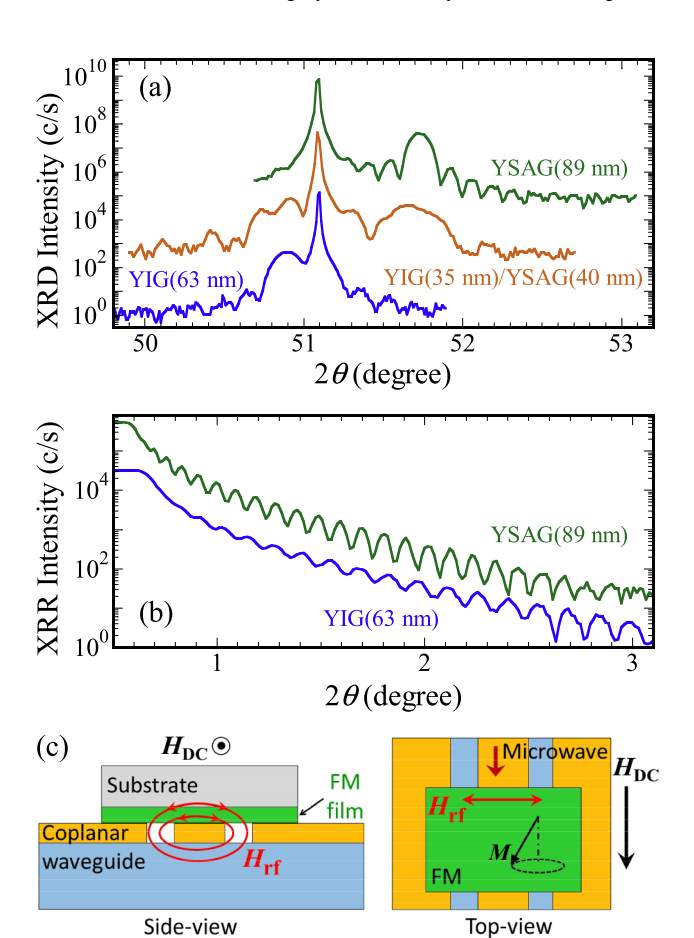


Fig. 1. (a) $2\theta/\omega$ XRD scans of YIG(63 nm)/GGG(111), YSAG(89 nm)/GGG (111) and YIG(35 nm)/YSAG(40 nm)/GGG(111) films. (b) XRR scans of YIG (63 nm)/GGG and YSAG(89 nm)/GGG films. (c) Schematic of broadband FMR measurement with both the side view and the top view.

films, and the XRR periodic peaks reveal the film thickness and low interfacial and surface roughness. For the YSAG (89 nm) film, the (444) peak is located at $2\theta = 51.728^{\circ}$, corresponding to an out-of-plane lattice constant of 12.210 Å, which is smaller than the bulk lattice constant of a = 12.344 Å due to tensile strain on GGG. Scanning transmission electron microscopy (STEM) images from our previous reports on the magnetic garnet and YSAG films [25,26] also show single crystal ordering without detectable defects in our epitaxial garnet films. From the symmetrical shape of the YSAG(444) XRD peak and previous STEM images, it appears that the YSAG layer is essentially fully strained (tensile), meaning that its in-plane lattice constant is the same as that of GGG while the outof-plane lattice constant is reduced. Consequently, the YIG film grown on the YSAG buffer layer will have the same, negligible lattice mismatch as YIG directly grown on GGG. In this work, we focus on three samples: a YIG(35 nm) film directly grown on GGG (111), YIG(35 nm)/YSAG(2 nm)/GGG (111) and YIG(35 nm)/YSAG(5 nm)/GGG (111).

Broadband FMR measurement is performed on the three YIG samples in a Physical Property Measurement System (PPMS) from Quantum Design, which allows control of magnetic field and temperature in the range 2–300 K. The garnet film is placed on a coplanar waveguide (CPW) that transmits microwave of frequency between 5 and 20 GHz. Fig. 1c gives a schematic of the broadband FMR measurement setup. The microwave's radio-frequency (rf) magnetic field component drives the precession of the YIG magnetization. An in-plane DC magnetic field is applied to the sample together with a modulating field for lock-in detection of the microwave absorption, from which a derivative FMR spectrum is obtained.

Fig. 2a-2c show three representative derivative FMR spectra for YIG (35 nm)/GGG measured at 300, 45, and 2 K with a microwave frequency of 10 GHz. The resonance field $H_{\rm r}$ and linewidth ΔH are extracted from fitting the lineshapes with.

$$y = [A - B(H - H_{\rm r})] / \left[(H - H_{\rm r})^2 + (\Delta H / 2)^2 \right]^2$$
 (2)

where A and B are the symmetric and antisymmetric amplitudes of the lineshape, respectively.

3. Results and discussion

According to the LLG equation, the FMR linewidth is linearly dependent on the microwave frequency, with the slope determined by the phenomenological Gilbert damping coefficient α :

$$\Delta H = 4\pi \alpha f / \gamma + \Delta H_0 \tag{3}$$

where ΔH_0 is the inhomogeneous broadening determined by the yintercept, which is generally attributed to magnetic nonuniformity [27] and surface defects [28]. In Fig. 2a-2c, as the temperature decreases from 300 K to 45 K and 2 K, the FMR linewidth for YIG(35 nm)/GGG increases while the peak intensity of FMR absorption decreases, suggesting enhanced damping at lower temperatures. Meanwhile, the resonant field of the YIG film decreases at lower temperatures, indicating an increasing effective magnetization, which agrees with our previous report [29]. Fig. 2d shows the frequency dependence of the fitted linewidth at various temperatures between 2 and 300 K, where the FMR linewidth exhibits a linear dependence on frequency with the slope increasing toward the lower temperatures. Fig. 2e and 2f show the temperature dependence of the damping α and inhomogeneous broadening ΔH_0 extracted from Eq. (3) for the YIG/GGG sample. The damping constant increases monotonically with decreasing temperature from 4.1 imes 10⁻⁴ at room temperature to 5.9 imes 10⁻³ at 2 K, a drastic increase of 14 times. Meanwhile, the inhomogeneous broadening also increases sharply from $\Delta H_0 = 0.69$ Oe at room temperature to 39 Oe at 2 K.

To understand the contributions to the YIG damping at low temperatures, we use a diamagnetic, lattice-matched YSAG buffer layer to separate the YIG film from the GGG substrate. Since the magnetic coupling between the YIG magnetization and the Gd^{3+} moments at low

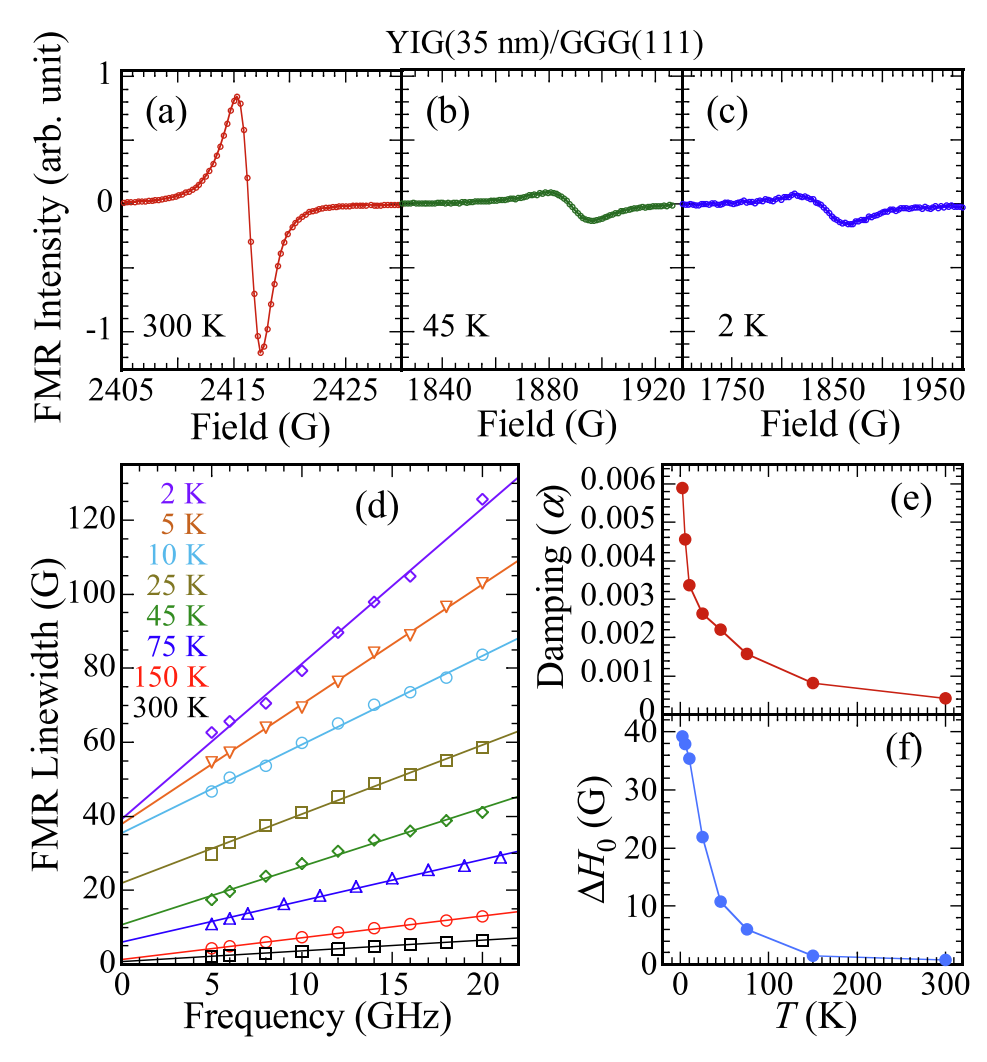


Fig. 2. Derivative FMR spectra of the YIG(35 nm)/GGG(111) sample measured at (a) 300 K, (b) 45 K and (c) 2 K, with a microwave frequency of 10 GHz. (d) Frequency dependencies of fitted FMR linewidths of YIG(35 nm)/GGG at various temperatures. Temperature dependencies of (e) damping and (f) inhomogeneous broadening of YIG(35 nm)/GGG obtained from linear fits to the variation of the linewidth vs frequency.

temperatures is dominated by interfacial exchange interactions, a few nm thick YSAG spacer is sufficient to isolate the two. We grow and perform the same broadband FMR measurement on YIG(35 nm)/YSAG (2 nm)/GGG and YIG(35 nm)/YSAG(5 nm)/GGG samples at temperatures between 2 and 300 K as shown in Fig. 3a and 3b, respectively, from which the damping constant and inhomogeneous broadening are extracted.

Fig. 4 compares the two YIG films grown on YSAG buffer layers to the YIG film grown directly on GGG. From Fig. 4a, we notice that the FMR linewidths at 5–20 GHz for both YIG/YSAG/GGG samples are essentially the same as those for YIG/GGG at 300 K, again proving the excellent quality of YIG films on buffer layers. However, the FMR linewidths for the two YIG/YSAG/GGG samples are considerably lower than those for YIG/GGG at 2 K (Fig. 4b), indicating that the thin YSAG buffer layer significantly reduces the damping loss in YIG films at low temperatures.

Fig. 4c and 4d compare the temperature dependence of damping constant and inhomogeneous broadening for all three samples. We note that the linewidth vs frequency dependence shows nonlinearity at temperatures from $10\sim75\,\mathrm{K}$, a phenomenon that is known to arise from slowly relaxing rare earth impurities in YIG [11,18–20]. This can be described in terms of a frequency-dependent damping constant that requires physics going beyond the simple Gilbert damping model embodied in Eq. (1). Nonetheless, the frequency dependence of linewidth here is linear enough above 5 GHz that the damping constant α provides a good estimate of the damping magnitude. Thus, the damping

constant used here is a simplistic figure of merit obtained from the data above 5 GHz, which reflects the intensity of relaxation within the films, and the true picture is more complicated. At 300 K, the three samples have essentially the same damping constant of $3.6\text{--}4.1\times10^{-4}$, consistent with variations of substrate and film quality, demonstrating that the YSAG buffer layer preserves the crystalline and magnetic quality of the overlaying YIG film. As the temperature decreases to below 100 K, the damping constants of the YIG/YSAG/GGG samples deviate qualitatively from that of YIG/GGG, where the former peaks around 20–45 K followed by a decrease towards 1×10^{-3} while the latter increases sharply approaching 6×10^{-3} .

The peaking of damping around 20–45 K for the YIG/YSAG/GGG samples in Fig. 4c is commonly ascribed to the existence of slow relaxation mechanism through rare-earth impurities in the YIG films [11,18–20]. The absence of the peak in the YIG/GGG damping is likely due to the strength of the YIG/GGG interfacial exchange coupling that overwhelms the influence of slowly relaxing impurities in YIG, compared to the dramatic increase in damping loss of YIG magnetization through its coupling to Gd³⁺ moments across the interface as temperature approaches a few K. Moreover, the qualitative similarity of the YIG (35 nm)/YSAG(2 nm)/GGG and YIG(35 nm)/YSAG(5 nm)/GGG results indicates that the coupling arises from short-range exchange coupling rather than the long-range dipole coupling and is therefore independent of the buffer layer thickness beyond 2 nm. We conclude that the YIG/GGG interfacial exchange coupling is the dominant source of damping in

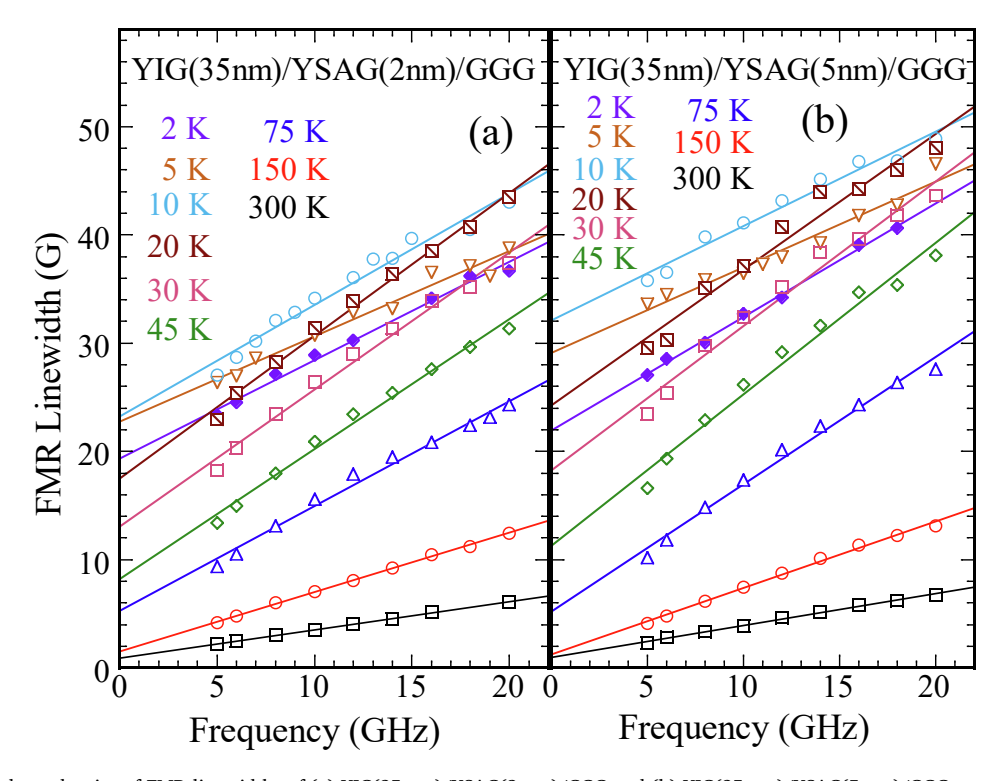


Fig. 3. Frequency dependencies of FMR linewidths of (a) YIG(35 nm)/YSAG(2 nm)/GGG and (b) YIG(35 nm)/YSAG(5 nm)/GGG at various temperatures.

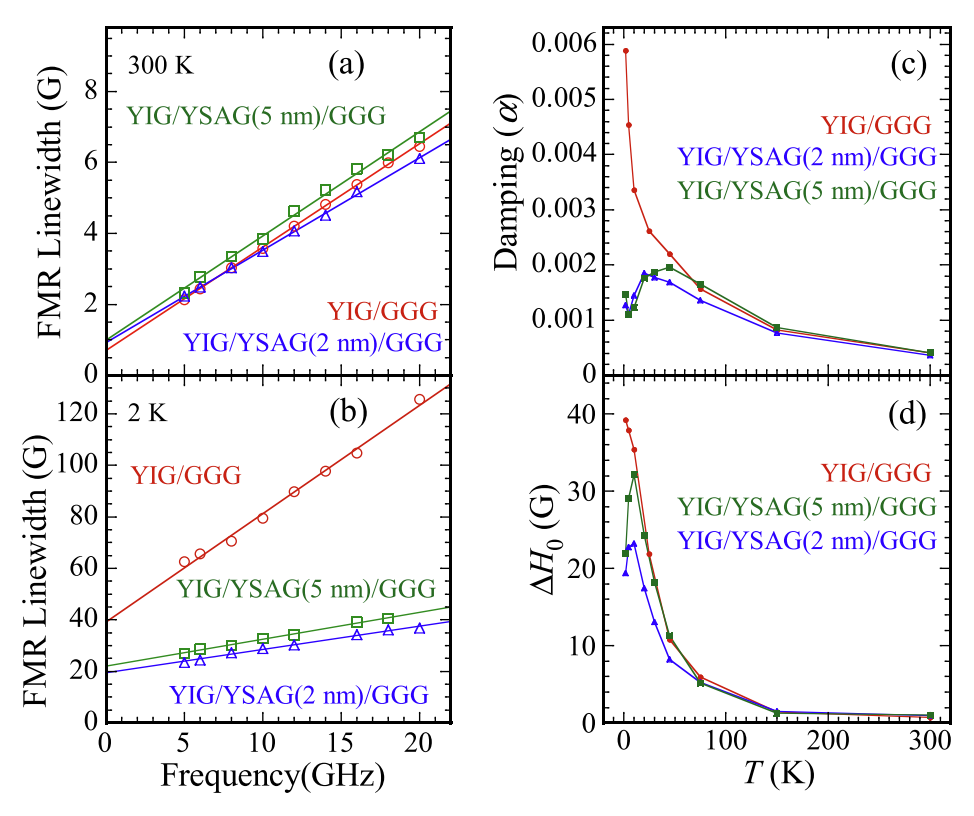


Fig. 4. Frequency dependencies of FMR linewidth for all three samples: YIG(35 nm)/GGG, YIG(35 nm)/YSAG(2 nm)/GGG, and YIG(35 nm)/YSAG(5 nm)/GGG at (a) 300 K and (b) 2 K. Temperature dependencies of (c) damping and (d) inhomogeneous broadening of the three samples.

the YIG film at several K; elimination of this interfacial coupling greatly reduces the damping constant at cryogenic temperatures.

Fig. 4d shows that the temperature dependencies of the inhomogeneous broadening is similar for the three samples from room

temperatures down to 10 K, but below this the YIG/YSAG/GGG samples exhibit a sharp decrease of ΔH_0 while YIG/GGG continues to increase. Since the YIG/GGG interfacial exchange coupling dominates below 10 K, it appears that this dominant source of relaxation is related to that

underlying the inhomogeneous broadening, although the exact mechanism for this behavior is unclear. We also notice the difference between the YIG/YSAG(2 nm)/GGG and YIG/YSAG(5 nm)/GGG samples, where YIG/YSAG(5 nm)/GGG has slightly broader FMR linewidths and inhomogeneous broadening. We tentatively attribute this to the fact that thicker buffer layer can have more defects, which can contribute to the nonuniformity of the film.

4. Summary

In summary, we grow high-quality epitaxial YIG films on a thin diamagnetic $\rm Y_3Sc_{2.5}Al_{2.5}O_{12}$ buffer layer on GGG (111) substrates. The YIG linewidth and damping at cryogenic temperatures are significantly improved compared to those of the YIG film directly grown on GGG. The significantly smaller damping in YIG/YSAG/GGG at low temperatures is attributed to the decoupling of the YIG magnetization from the Gd³⁺ moments in the GGG substrate across the interface, eliminating a strong source of damping. The introduction of a diamagnetic buffer layer that is nearly ideally matched to YIG as well as GGG can be readily incorporated into the large scale sputter deposition of YIG films. A very low damping constant at cryogenic temperatures greatly enhances the prospects for the application of YIG films in magnonics and quantum information science that require low temperatures.

Declaration of Competing Interest

The authors declare that they have no known competing financial interests or personal relationships that could have appeared to influence the work reported in this paper.

Data availability

Data will be made available on request.

Acknowledgement

This work was primarily supported by the Center for Emergent Materials, an NSF MRSEC, under Grant No. DMR-2011876. We acknowledge the technical assistance of Suyuan Liu. This article is dedicated to Chia-Ling Chien, who is an extraordinary mentor and a brilliant experimental physicist.

Author contribution

S.D.G. performed sample growth and characterization, FMR measurements and analysis, and manuscript writing. B.M. participated in FMR measurements. P.C.H. and F.Y.Y. supervised the project. All authors contributed to manuscript writing and revision.

References

- A.A. Serga, A.V. Chumak, B. Hillebrands, YIG magnonics, J. Phys. D-Appl. Phys. 43 (2010), 264002.
- [2] A.V. Chumak, V.I. Vasyuchka, A.A. Serga, B. Hillebrands, Magnon spintronics, Nat. Phys. 11 (2015) 453–461.
- [3] L.J. Cornelissen, J. Liu, R.A. Duine, J.B. Youssef, B.J. van Wees, Long-distance transport of magnon spin information in a magnetic insulator at room temperature, Nat. Phys. 11 (2015) 1022–1026.
- [4] A.V. Chumak, A.A. Serga, B. Hillebrands, Magnon transistor for all-magnon data processing, Nat. Commun. 5 (2014) 4700.

- [5] K. Vogt, F.Y. Fradin, J.E. Pearson, T. Sebastian, S.D. Bader, B. Hillebrands, A. Hoffmann, H. Schultheiss, Realization of a spin-wave multiplexer, Nat. Commun. 5 (2014) 3727.
- [6] L.J. Cornelissen, K.J.H. Peters, G.E.W. Bauer, R.A. Duine, B.J. van Wees, Magnon spin transport driven by the magnon chemical potential in a magnetic insulator, Phys. Rev. B 94 (1) (2016), https://doi.org/10.1103/PhysRevB.94.014412.
- [7] L. Sheng, J. Chen, H. Wang, H. Yu, Magnonics Based on Thin-Film Iron Garnets, J. Phys. Soc. Jpn 90 (8) (2021) 081005, https://doi.org/10.7566/JPSJ.90.081005.
- [8] M.Z. Wu, A. Hoffmann, Recent Advances in Magnetic Insulators From Spintronics to Microwave Applications, Academic Press, 2013.
- [9] G. Schmidt, C. Hauser, P. Trempler, M. Paleschke, E.T. Papaioannou, Ultra Thin Films of Yttrium Iron Garnet with Very Low Damping: A Review, Phys. Status Solidi B 257 (2020) 1900644.
- [10] F.Y. Yang, P.C. Hammel, Topical review: FMR-Driven Spin Pumping in $Y_3Fe_5O_{12}$ -Based Structures, J. Phys. D: Appl. Phys. 51 (2018), 253001.
- [11] C.L. Jermain, S.V. Aradhya, N.D. Reynolds, R.A. Buhrman, J.T. Brangham, M. R. Page, P.C. Hammel, F.Y. Yang, D.C. Ralph, Increased low-temperature damping in yttrium iron garnet thin films, Phys. Rev. B 95 (17) (2017), https://doi.org/10.1103/PhysRevB 95 174411
- [12] D. Lachance-Quirion, Y. Tabuchi, A. Gloppe, K. Usami, Y. Nakamura, Hybrid quantum systems based on magnonics, Appl. Phys. Express 12 (7) (2019) 070101, https://doi.org/10.7567/1882-0786/ab248d.
- [13] A.A. Clerk, K.W. Lehnert, P. Bertet, J.R. Petta, Y. Nakamura, Hybrid quantum systems with circuit quantum electrodynamics, Nat. Phys. 16 (2020) 257–267.
- [14] P.G. Baity, D.A. Bozhko, R. Macêdo, W. Smith, R.C. Holland, S. Danilin, V. Seferai, J. Barbosa, R.R. Peroor, S. Goldman, U. Nasti, J. Paul, R.H. Hadfield, S. McVitie, M. Weides, Strong magnon–photon coupling with chip-integrated YIG in the zero-temperature limit, Appl. Phys. Lett. 119 (2021), 033502.
- [15] Y. Li, V.G. Yefremenko, M. Lisovenko, C. Trevillian, T. Polakovic, T.W. Cecil, P. S. Barry, J. Pearson, R. Divan, V. Tyberkevych, C.L. Chang, U. Welp, W.-K. Kwok, V. Novosad, Coherent Coupling of Two Remote Magnonic Resonators Mediated by Superconducting Circuits, Phys. Rev. Lett. 128 (2022), 047701.
- [16] I.W. Haygood, M.R. Pufall, E.R.J. Edwards, J.M. Shaw, W.H. Rippard, Strong Coupling of an FeCo Alloy with Ultralow Damping to Superconducting Co-planar Waveguide Resonators, Phys. Rev. Appl. 15 (2021), 054021.
- [17] S.V. Vonsovskii, Ferromagnetic Resonance: The Phenomenon of Resonant Absorption of a High-Frequency Magnetic Field in Ferromagnetic Substances, Pergamon, 1966.
- [18] H. Maier-Flaig, S. Klingler, C. Dubs, O. Surzhenko, R. Gross, M. Weiler, H. Huebl, S. T.B. Goennenwein, Temperature-dependent magnetic damping of yttrium iron garnet spheres, Phys. Rev. B 95 (21) (2017), https://doi.org/10.1103/PhysRevB.95.214423.
- [19] P.E. Seiden, Ferrimagnetic Resonance Relaxation in Rare-Earth Iron Garnets, Phys. Rev. 133 (3A) (1964) A728–A736.
- [20] E.G. Spencer, R.C. LeCraw, A.M. Clogston, Low-Temperature Line-Width Maximum in Yttrium Iron Garnet, Phys. Rev. Lett. 3 (1959) 32–33.
- [21] L. Wang, Z. Lu, X. Zhao, W. Zhang, Y. Chen, Y. Tian, S. Yan, L. Bai, M. Harder, Magnetization coupling in a YIG/GGG structure, Phys. Rev. B 102 (14) (2020), https://doi.org/10.1103/PhysRevB.102.144428.
- [22] S. Kosen, A.F. van Loo, D.A. Bozhko, L. Mihalceanu, A.D. Karenowska, Microwave magnon damping in YIG films at millikelvin temperatures, APL Mater. 7 (2019), 101120.
- [23] L. Mihalceanu, V.I. Vasyuchka, D.A. Bozhko, T. Langner, A.Y. Nechiporuk, V. F. Romanyuk, B. Hillebrands, A.A. Serga, Temperature-dependent relaxation of dipole-exchange magnons in yttrium iron garnet films, Phys. Rev. B 97 (21) (2018), https://doi.org/10.1103/PhysRevB.97.214405.
- [24] O. Opuchovic, A. Kareiva, K. Mazeika, D. Baltrunas, Magnetic nanosized rare earth iron garnets R₃Fe₅O₁₂: Sol-gel fabrication, characterization and reinspection, J. Magn. Magn. Mater. 422 (2017) 425–433.
- [25] A.S. Ahmed, A.J. Lee, N. Bagués, B.A. McCullian, A.M.A. Thabt, A. Perrine, P.-K. Wu, J.R. Rowland, M. Randeria, P.C. Hammel, D.W. McComb, F. Yang, Spin-Hall Topological Hall Effect in Highly Tunable Pt/Ferrimagnetic-Insulator Bilayers, Nano Letters 19 (8) (2019) 5683–5688.
- [26] A.J. Lee, S.D. Guo, J. Flores, B.B. Wang, N. Bagués, D.W. McComb, F.Y. Yang, Investigation of the Role of Rare-Earth Elements in Spin-Hall Topological Hall Effect in Pt/Ferrimagnetic-Garnet Bilayers, Nano Letters 20 (2020) 4667–4672.
- [27] E. Schlömann, Inhomogeneous Broadening of Ferromagnetic Resonance Lines, Phys. Rev. 182 (1969) 632–645.
- [28] S. Klingler, H. Maier-Flaig, C. Dubs, O. Surzhenko, R. Gross, H. Huebl, S.T. B. Goennenwein, M. Weiler, Gilbert damping of magnetostatic modes in a yttrium iron garnet sphere, Appl. Phys. Lett. 110 (2017), 092409.
- [29] J.C. Gallagher, A.S. Yang, J.T. Brangham, B.D. Esser, S.P. White, M.R. Page, K. Y. Meng, S.S. Yu, R. Adur, W. Ruane, S.R. Dunsiger, D.W. McComb, F.Y. Yang, P. C. Hammel, Exceptionally high magnetization of stoichiometric Y₃Fe₅O₁₂ epitaxial films grown on Gd₃Ga₅O₁₂, Appl. Phys. Lett. 109 (2016), 072401.